Journal of Solid State Chemistry **157,** 23–29 (2001)
doi:10.1006/jssc.2000.9021, available online at http://www.idealibrary.com on IDEAL®

$Cu_xM_{1-x}(HCOO)_2 \cdot 2H_2O$, ($M$=Mn, Co, Ni, Cd): Crystal Structures and Thermal Behavior

A. G. Leyva,[1] G. Polla, D. Vega, R. Baggio, P. K. de Perazzo, M. A. R. de Benyacar, and M. T. Garland*

*Dpto de Fisica, CNEA, Avda Gral Paz 1499, 1650 San Martin, Buenos Aires, Argentina; and *Dpto de Fisica, Fac.de Ciencias Fisicas y Matemáticas, U. de Chile, Av. Blanco Encalada 2008, Caja Postal 487-3, Santiago, Chile*

Received May 12, 2000; in revised form October 5, 2000; accepted November 6, 2000

A crystallographic and thermal study of the system $Cu_xM_{1-x}(HCOO)_2 \cdot 2H_2O$ (M:Mn, x=0.47; Co, x=0.35; Ni, x=0.37; Cd, x=0.47) has been performed. The compounds, grown at room temperature, crystallize in space group $P2_1/c$ and are isostructural with $Cu_{0.5}Zn_{0.5}(HCOO)_2 \cdot 2H_2O$ (1), with the cations sharing the two special position sites M1 and M2. In all cases, the best refinement was achieved with the copper atoms occupying preferentially the hexaformate-coordinated site M1, while the M^{2+} cations were mainly localized in the M2 sites, in a mixed coordination environment. The compounds present a variety of thermal behaviors, with dehydration taking place at different temperatures and decomposition going from a simple single step process, as in the Zn compound, up to a complex three-stage one as in the Mn and Cd compounds. Decomposition products were identified by X-ray diffraction on quenched samples at the end of each thermal stage. Some discrepancies of the present results with those in the literature are discussed.

Key Words: **$Cu_xM_{1-x}(HCOO)_2 \cdot 2H_2O$ (M:Mn, x=0.47; Co, x=0.35; Ni, x=0.37; Cd, x=0.47) crystal structure; thermal behavior.**

INTRODUCTION

The system of isostructural mixed formates of general formula $Cu_xM_{1-x}(HCOO)_2 \cdot 2H_2O$ (M divalent metals) has been extensively studied since the late 1970s, due to its peculiar properties: crystallographic data and IR measurements seemed to indicate a nonuniform distribution of the two cations between the two lattice sites in the Cu–Zn (1, 2), Cu–Mg, and Cu–Cd systems (3 and references therein) and Cu–Mn (4). Controversial hypotheses abound, however, about the way in which, and the reasons why, this phenomenon took place: in the Cu–Zn and Cu–Mn cases, the Cu^{2+} ions were reported to exhibit a clear preference for the hexaformate coordinated site (hereafter M1); diffuse reflectance spectroscopy experiments in the visible range performed on $Cu_xCd_{1-x}HCOO_2 \cdot 2H_2O$ (3), $Cu_xZn_{1-x}HCOO_2 \cdot 2H_2O$ (5), and $Cu_xCo_{1-x}HCOO_2 \cdot 2H_2O$ (6) mixed crystals, however, have been interpreted as to provide evidence for the preferential incorporation of the Cu^{2+} ions in the mixed coordination environment (hereafter M2). Pursuant our interest in mixed copper formate systems, and in order to contribute to the clarification of this still open issue, we here report a thermal and crystallographic structural study of compounds of the system $Cu_xM_{1-x}(HCOO)_2 \cdot 2H_2O$ (M:Mn, $x = 0.47$; Co, $x = 0.35$; Ni, $x = 0.37$; Cd, $x = 0.47$). The detailed structural study of the zinc compound was omitted, since its X-ray crystal structure for $x = 0.50$ had already been reported (1).

EXPERIMENTAL

Crystals of $Cu_xM_{1-x}HCOO_2 \cdot 2H_2O$ [M = Mn(**i**), Co(**ii**), Ni(**iii**), Cd (**iv**), and Zn] were grown by slow evaporation at room temperature starting from 1:1 (Cu:M) proportions of $CuCO_3 \cdot Cu(OH)_2$ and the corresponding metal carbonates or nitrates in 20% aqueous formic acid solution. To avoid important changes in the cation concentration of the solution, crystals were filtrated as soon as they appeared. In spite of the fact that in all the compounds the 1:1 Cu/M ratios were checked using a flame atomic absorption analysis instrument (Jarrell Ash Model 82-500), the ultimate incorporation of Cu to the crystal structures was in all cases smaller than expected, as confirmed by both chemical analysis of the bulk as well as EDAX analysis on individual single crystals. The later gave, in addition, a rough idea of a low dispersion of concentrations in the samples.

The thermal experiments were carried out with simultaneous measurements of thermogravimetry and differential thermal analysis in a DTG-50/50 H Shimadzu apparatus,

[1]To whom corresppondence should be addressed.

0022-4596/01 $35.00

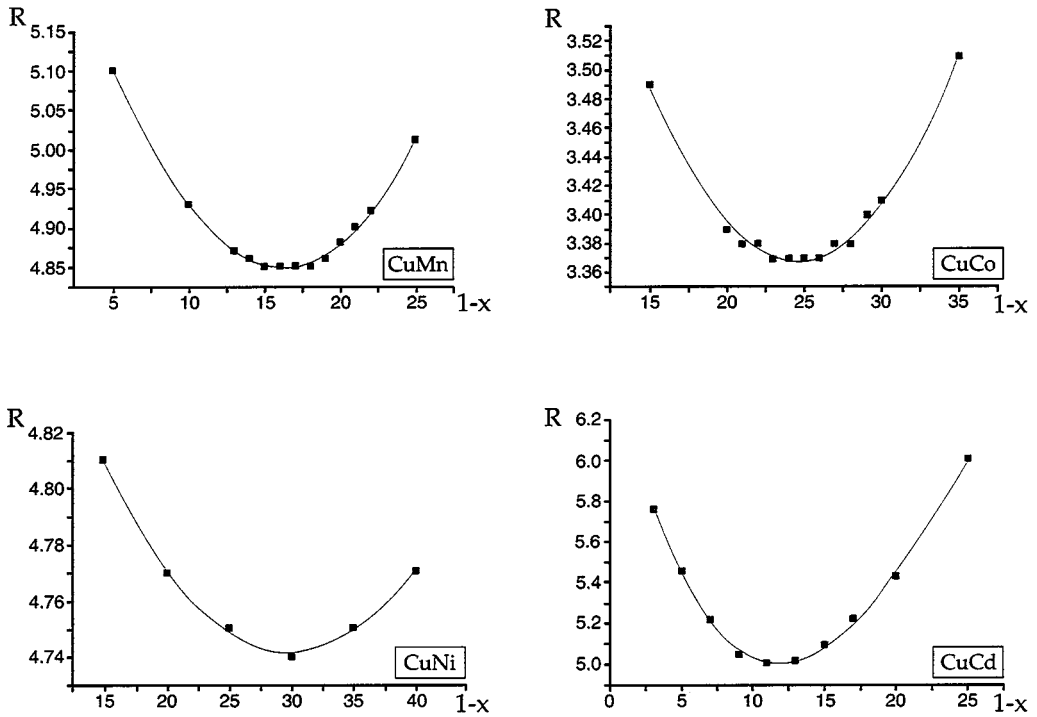

FIG. 1. Behavior of the least squares refinement agreement factor (R) as a function of the concentration of cation M at site M1, $(1 - x)$, for **(i)**, **(ii)**, **(iii)**, and **(iv)**.

between 30 and 1000°C, in air, at a heating rate of 10°C/min. Each sample was pulverized in an agate mortar in order to carry out the thermal treatments under the same conditions for all the mixed formates. The decomposition products were identified by X-ray diffraction at ambient temperature, on a Philips PW-3710 diffractometer (Cu$K\alpha$ radiation, $\lambda = 1.5418$ Å) using quenched samples at the different stages of the decomposition.

Medium-sized crystals invariably proved useless for single-crystal X-ray diffraction experiments, probably due to some kind of twinning which made impossible the finding of a proper unit cell in the single-crystal diffractometer. Very

TABLE 1
Crystal Data for (i), (ii), (iii), and (iv)

Formula	$C_2H_6Cu_{0.47}Mn_{0.53}O_6$ **(i)**	$C_2H_6Co_{0.65}Cu_{0.35}O_6$ **(ii)**	$C_2H_6Cu_{0.37}Ni_{0.63}O_6$ **(iii)**	$C_2H_6Cd_{0.53}Cu_{0.47}O_6$ **(iv)**
M	185.31	187.30	187.19	214.04
Crystal size (mm)	$0.14 \times 0.14 \times 0.08$	$0.17 \times 0.17 \times 0.07$	$0.16 \times 0.14 \times 0.10$	$0.15 \times 0.15 \times 0.08$
a (Å)	8.844(4)	8.802(3)	8.740(4)	8.773(4)
b(Å)	7.236(2)	7.187(2)	7.127(3)	7.223(2)
c(Å)	9.311(4)	9.124(3)	9.096(4)	9.485(3)
β	97.36(3)	97.72(2)	97.88(4)	96.61(3)
U(Å^3)	590.9(4)	572.0(3)	561.2(4)	597.1(4)
Dc (g cm^{-3})	2.08	2.17	2.22	2.38
F (000)	372	376	378	418
μ (mm^{-1})	2.92	3.37	363	3.62
Data/parameters ratio	9.46	9.15	9.01	9.61
$R1^a$, w$R2^b$ $[I > 2\sigma(I)]$	0.049, 0.095	0.035, 0.074	0.048, 0.104	0.049, 0.100
Maximum difference peak, hole/e Å^{-3}	0.52, −0.56	0.39, −0.38	1.03, −0.50	0.82, −0.72

Note. Details in common: T, 293 K; monoclinic, $P2(1)/c$ (No. 14); small hexagonal plates, $z = 4$; 2θ upper limit, 50°; lambda (Mo$K\alpha$): 0.7107 Å; absorption correction, psi scan.

[a] $R1 = \sum ||F_o| - |F_c|| / \sum |F_o|$.

[b] $wR2 = [\sum [w(F_o^2 - F_c^2)^2] / \sum [w(F_o^2)^2]]^{1/2}$.

TABLE 2
Atomic Coordinates, Equivalent Isotropic Displacement Factors, and Site Occupation Factors for (i), (ii), (iii), and (iv)

Compound	Atom	*x/a*	*y/b*	*y/c*	U_{eq} (Å^{-2})	S.O.F.
(i)	Cu1/Mn1	0.0000	0.0000	0.0000	0.0197(5)	0.68/0.32
	Mn2/Cu2	0.5000	0.5000	0.0000	0.0263(6)	0.74/0.26
	C1	0.0366(12)	0.2242(15)	0.2789(12)	0.031(3)	1
	O1	0.0944(7)	0.1057(10)	0.2092(7)	0.0299(19)	1
	O2	0.0865(7)	0.2766(98)	0.4054(7)	0.0306(17)	1
	C2	0.3224(13)	0.6147(15)	0.4382(11)	0.031(3)	1
	O3	0.4346(8)	0.7180(10)	0.4240(7)	0.0356(18)	1
	O4	0.2101(7)	0.6597(9)	0.4993(7)	0.0312(17)	1
	O1W	0.2744(8)	0.4789(18)	0.0700(8)	0.035(2)	1
	O2W	0.4092(10)	0.1065(16)	0.2969(8)	0.052(3)	1
(ii)	Cu1/Co1	0.0000	0.0000	0.0000	0.0146(3)	0.52/0.48
	Co2/Cu2	0.5000	0.5000	0.0000	0.0193(‘3)	0.82/0.18
	C1	0.0364(7)	0.2265(9)	0.2742(6)	0.0250(14)	1
	O1	0.0950(4)	0.1035(5)	0.2033(4)	0.0218(9)	1
	O2	0.0890(4)	0.2791(6)	0.4015(4)	0.0221(9)	1
	C2	0.3254(7)	0.6224(10)	0.4405(6)	0.0278(14)	1
	O3	0.4372(5)	0.7252(6)	0.4253(4)	0.0293(10)	1
	O4	0.2125(5)	0.6657(6)	0.5030(4)	0.0275(10)	1
	O1W	0.2827(5)	0.4717(6)	0.0748(5)	0.0242(10)	1
	O2W	0.4113(6)	0.1020(8)	0.2981(5)	0.0390(13)	1
(iii)	Cu1/Ni1	0.0000	0.0000	0.0000	0.0168(3)	0.40/0.60
	Ni2/Cu2	0.5000	0.5000	0.0000	0.0225(3)	0.66/0.34
	C1	0.0350(7)	0.2269(10)	0.2730(7)	0.0260(15)	1
	O1	0.0944(6)	0.1039(6)	0.2018(5)	0.0237(10)	1
	O2	0.0891(5)	0.2802(6)	0.4023(5)	0.0243(10)	1
	C2	0.3260(9)	0.6212(12)	0.4413(8)	0.0336(18)	1
	O3	0.4372(6)	0.7250(8)	0.4227(5)	0.0392(13)	1
	O4	0.2117(5)	0.6644(7)	0.5029(5)	0.0312(12)	1
	O1W	0.2881(7)	0.4718(7)	0.0732(6)	0.0286(11)	1
	O2W	0.4129(6)	0.1060(10)	0.3016(6)	0.0445(16)	1
(iv)	Cu1/Cd1	0.0000	0.0000	0.0000	0.0233(4)	0.76/0.24
	Cd2/Cu2	0.5000	0.5000	0.0000	0.0298(4)	0.82/0.18
	C1	0.0373(16)	0.2227(19)	0.2882(17)	0.037(3)	1
	O1	0.0987(9)	0.1092(11)	0.2169(9)	0.034(2)	1
	O2	0.0870(9)	0.2769(11)	0.4098(7)	0.0295(18)	1
	C2	0.3194(16)	0.6059(19)	0.4356(14)	0.035(3)	1
	O3	0.4312(10)	0.7039(11)	0.4195(9)	0.039(2)	1
	O4	0.2061(9)	0.6500(11)	0.4945(8)	0.0312(19)	1
	O1W	0.2688(11)	0.4836(19)	0.0740(9)	0.038(2)	1
	O2W	0.4089(15)	0.116(2)	0.2986(13)	0.062(4)	1

small specimens, instead, were readily centered in spite of the reduced diffracted intensity and were accordingly chosen for data collection on a Siemens R3 diffractometer (Mo$K\alpha$ radiation, $\lambda = 0.7107$ Å).

RESULTS

The starting model used for the structure resolution was the one reported in (1). Refinement on F^2 using SHELXL97 (7) with fixed occupancies for copper and *M* as given by the chemical analysis and assuming equidistribution over both special positions M1 and M2 (multiplicity 0.5) readily converged to a low *R* factor. When the occupation factors were allowed to vary, however, preserving the constraints imposed by the known chemical composition (Cu_xM_{1-x}, site M1; $Cu_yM_{0.5-y}$, site M2; $Cu_z,M_{0.5-z}$, $y + z = x$) very high correlations with the anisotropic temperature factors were found, which prevented the obtention of trustable results. It was then decided to make a series of refinements at closely spaced intervals of the fixed copper occupation factors *x*. From the minimum of the *R* vs $(1 - x)$ curve thus obtained (Fig. 1), a good estimate of the parameter *x* could be obtained, while an estimate of the uncertainty could be found from the second derivative of the curve. As expected, the larger the difference in atomic number between the two cations, the steeper was the curve and better defined appeared the occupation (extreme cases; cadmium ($\Delta z = 19$); nickel ($\Delta z = 1$)). The latter case, though poorly defined, could be clearly fitted in a general trend to be discussed below.

Structural Analysis

As previously mentioned in the experimental section, the structures herein reported are isostructural to the Cu–Zn homologs already described in the literature (1), and therefore they will not be discussed in detail. Tables 1, 2, and 3 display in a compact way a composition of crystal data, displacement factors, site occupation factors, and coordination distances among the mixed formates dihydrates presented in this work (labeled Cu*M*). Relevant information for the pure formates (*M*) from where they derive is also presented. As we can see copper ions in all the compounds studied exhibit a clear preference for the hexaformate coordinated site M1. As expected, the aqua molecules are fully engaged in H-bonding, as shown in Table 4. The sole exception is O1W in (iv), which has only one hydrogen, H1WB, involved in such interactions, H1WA being too far from any possible acceptor.

Thermal Behavior

The TGA curves of the mixed formates dihydrates are shown in Fig. 2. The temperature range of dehydration and decomposition processes as well as the weight loss after each stage are listed in Table 5. The good agreement between calculated and experimental values of weight loss indicate that the dehydration process for all the mixed Cu–*M* dihydrated formates studied takes place in one well-differentiated stage after which the decomposition process starts.

X-ray diffraction patterns on quenched samples after the dehydration stage (*M* = Mn, Co, Zn) are very similar, and cannot be fitted (not even partially) to any of the reported simple formates. The absence in the diagrams of the characteristic peaks of the well known copper formate, make us believe that the phase corresponds to an unreported mixed formate. The poor quality of X-ray data obtained (broad peaks mounted onto a high background) precluded a more profound analysis, but work on the subject is in progress. In

TABLE 3
Selected Bond Distances (Å) and Angles for (i), (ii), (iii), and (iv). (Columns Labeled CuM) and for the Simple Formates from Where They Derive (Labeled M)

	M = Mn (**i**)		M = Co (**ii**)		M = Ni (**iii**)		M = Cd (**iv**)		M = Cu
	CuM	M	CuM	M	CuM	M	CuM	M	M
a (Å)	8.844(4)	8.86	8.802(3)	8.63	8.740(4)	8.60	8.773(4)	8.98	8.54
b (Å)	7.236(2)	7.18	7.187(2)	7.06	7.127(3)	7.06	7.223(2)	7.39	7.15
c (Å)	9.311(4)	9.39	9.124(3)	9.21	9.096(4)	9.21	9.485(3)	9.76	9.50
β (°)	97.36(3)	97.6	97.72(2)	96.0	97.88(4)	96.8	96.61(3)	97.3	96.8
% Of total copper composition x at sites M1/M2	70/30(6)		66/34(6)		56/44(9)		80/20(2)		
Cu(1)–O(2)#1	2.036(7)	2.135	2.032(4)	2.04	2.010(4)	2.026	2.015(7)	2.286	1.988
Cu(1)–O(1)	2.159(7)	2.172	2.068(4)	2.03	2.045(4)	2.061	2.279(8)	2.263	2.304
Cu(1)–O(4)#1	2.189(7)	2.218	2.215(4)	2.10	2.185(5)	2.097	2.113(8)	2.300	2.019
M(2)–O(2W)#2	2.103(8)	2.168	2.036(5)	2.07	2.006(6)	2.042	2.153(12)	2.242	1.974
M(2)–O(1W)	2.182(8)	2.216	2.124(4)	2.06	2.061(5)	2.059	2.226(10)	2.298	2.044
M(2)–O(3)#3	2.212(7)	2.219	2.138(4)	2.06	2.129(5)	2.090	2.326(8)	2.326	2.368
O(2)#4–Cu(1)–O(1)#5	90.8(3)		91.0(2)		91.1(2)		90.9(3)		
O(2)#4–Cu(1)–O(4)#4	93.0(3)		92.9(2)		92.6(2)		91.9(3)		
O(1)#5–Cu(1)–O(4)#4	92.3(3)		93.2(2)		93.1(2)		92.2(3)		
O(2W)#4–M(2)–O(1W)#6	90.9(3)		90.3(2)		90.4(2)		90.0(4)		
O(2W)#2–M(2)–O(3)#7	90.2(4)		90.4(2)		90.0(3)		90.5(4)		
O(1W)–M(2)–O(3)#3	92.9(4)		90.8(2)		90.3(2)		93.4(4)		

Note. Symmetry transformations used to generate equivalent atoms: #1, $-x, y-\frac{1}{2}, -z+\frac{1}{2}$; #2, $-x+1, y+\frac{1}{2}, -z+\frac{1}{2}$; #3, $-x+1, y-\frac{1}{2}, -z+\frac{1}{2}$; #4, $x, -y+\frac{1}{2}, z-\frac{1}{2}$; #5, $-x, -y, -z$; #6, $-x+1, -y+1, -z$; #7, $x, -y+\frac{3}{2}, z-\frac{1}{2}$.

the case of M = Ni both the dehydration as well as the decomposition processes take place at almost the same temperature, making almost impossible the identification of intermediate products. The case for M = Cd was the only one in which copper formate was detected as one of the dehydration products, the accompanying phase could be a phase of the anhydrous Cd formate. No powder data could be found in the literature to corroborate this point, but a simulated powder diagram from single crystal data (8) closely matches the unaccounted for peaks; thus confirming the original hypothesis.

Trials to obtain the anhydrous mixed formates by higher temperature synthesis proved so far unsuccessful.

After dehydration, further decomposition takes place in one stage for the Zn compound, in two stages for the Co, Mn, and Ni compounds, and in three stages for the Cd compound. Complete decomposition into the copper (II) oxide and the corresponding divalent metal oxides takes place after an oxidation process near 300°C for all the samples under study as confirmed by X-ray diffraction analysis of the quenched samples. When heating up to 1000°C, X-ray analysis of the quenched Mn, Co, and Ni compounds show, as the only crystalline phase present, different metal cuprates with varied stoichiometries (Table 5) according to the ICDD data base (9), thus suggesting a solid-state reaction at high temperatures. For Zn and Cd the corresponding cuprates were never found, the process ending up in the simple oxides.

DISCUSSION AND CONCLUSIONS

From X-ray diffraction analysis the M1–O and M2–O coordination distances in Table 3 can be reasonably explained, as a first approximation, as "effective values" obtained by the averages of the Cu–O and M–O respective values, weighted by their corresponding occupancies in both sites. For M = Mn, Co, and Ni, however, an extra requirement is needed to account for the values obtained, and it is that the apical bond of the copper coordination polyhedra must change direction with respect to that in the pure copper formate (1). In the case of M = Cd, this is not so, the orientation of both copper octahedra being similar. This could be ascribed to the fact that in the latter case there is a predominant copper content in site M1, thus giving it a definite "copper formate" character. If this is true, a change in the orientation of the polyhedron should be observed as the copper composition x changes from 1 to 0. For M = Zn it is stated in (1) that the copper coordination

TABLE 4
Hydrogen Bond Interactions in (i), (ii), (iii), and (iv)

M	O_d	H_d	$O_a^{\#sym}$	O_d–H_d (Å)	$H_d \cdots O_a$ (Å)	$O_d \cdots O_a$ (Å)	O_d–$H_d \cdots O_a$ (°)
Mn (**i**)							
	O2W	H2WA	$03^{\#1}$	0.77(4)	1.98(4)	2.74(1)	170(4)
	O2W	H2WB	$O1^{\#2}$	0.79(4)	2.03(3)	2.79(1)	160(3)
	O1W	H1WA	$O4^{\#3}$	0.83(5)	2.00(5)	2.74(1)	149(5)
	O1W	H1WB	$O2^{\#4}$	0.82(6)	2.01(6)	2.80(1)	162(6)
Co (**ii**)							
	O2W	H2WA	$O3^{\#1}$	0.76(4)	1.99(4)	2.73(1)	165(4)
	O2W	H2WB	$O1^{\#2}$	0.79(3)	2.02(3)	2.80(1)	170(3)
	O1W	H1WA	$O4^{\#3}$	0.82(3)	1.95(3)	2.74(1)	160(3)
	O1W	H1WB	$O2^{\#4}$	0.79(4)	2.03(4)	2.82(1)	168(4)
Ni (**iii**)							
	O2W	H2WA	$O3^{\#1}$	0.81(4)	1.90(04)	2.71(1)	175(4)
	O2W	H2WB	$O1^{\#2}$	0.84(3)	1.96(03)	2.80(1)	174(3)
	O1W	H1WA	$O4^{\#3}$	0.85(4)	1.97(03)	2.73(1)	147(3)
	O1W	H1WB	$O2^{\#4}$	0.83(4)	1.99(04)	2.81(1)	168(4)
Cd (**iv**)							
	O2W	H2WA	$O3^{\#1}$	0.79(5)	2.04(6)	2.70(1)	141(4)
	O2W	H2WB	$O1^{\#2}$	0.78(5)	2.06(4)	2.75(1)	148(4)
	O1W	H1WB	$O4^{\#3}$	0.77(5)	2.04(6)	2.80(1)	166(5)

Note. Symmetry transformations used to generate equivalent atoms: #1, $-x+1$, $y+0.5$, $-z+0.5$; #2, $-x+2$, $y+0.5$, $-z+0.5$; #3, $-x+1$, $-y+1$, $-z$; #4, $x-1$, $-y+0.5$, $z-0.5$.

polyhedron changes direction with respect to that in the pure copper formate, thus suggesting that the occupancy factor is lower than 80% for copper at site M1. Testing of these hypotheses, however, would require a series of controlled synthesis, crystal growth and structure determinations, a fact that is well beyond the scope of the present work.

The systematically lower dehydration temperatures of the Cu–M mixed formates as compared with those of the pure Mn, Co, and Ni formates from which they derive shows that incorporation of copper decreases the thermal stability of the structures: the copper ions that substitute for M^{2+} in these compounds could be considered as defects in the structure; a decrease in thermal stability has been recently observed in the manganese-containing oxides todorokite and cryptomelane, where it has been shown that the thermal stability of the crystal structures decreases as the amount of Cu that substitutes for Mn in the structure increases (10). On the other hand, the opposite tendency is observed when copper substitutes for zinc or cadmium in the structures of the pure cadmium or zinc dihydrated formates: the stability increases with the incorporation of copper in these structures, in good agreement with previous results for the Cu–Zn case (11).

The dehydration temperature of both the pure M and the mixed Cu–M compounds show the same behavior when represented, for example, as a function of the number of electrons in the Md orbitals, as seen in Fig. 3. In both families of compounds dehydration temperatures for M = Zn and Cd, which have filled d orbitals, are lower than dehydration temperatures for the Mn, Ni, and Co salts. As expected, in the latter case their partially filled orbitals contribute to a stronger bonding energy with the

TABLE 5
Weight Losses and Decomposition Products Detected during Thermal Decomposition of $Cu_xM_{(1-x)}(HCOO)_2 \cdot 2H_2O$ Compounds

Compound	Temperature range (°C)	Weight loss (%)	Main crystalline final products at $T = 1000$°C
$(Cu_{0.47}Mn_{0.53})(HCOO)_2 \cdot 2H_2O$	72–154	Experimental: 19.24	$Cu_{1.4}Mn_{1.6}O_4$
	T peak: 122	Calculated: 19.43	
	154–231	13.85	
	231–273	23.62	
$(Cu_{0.35}Co_{0.65})(HCOO)_2 \cdot 2H_2O$	83–160	Experimental: 19.35	$Cu_{0.92}Co_{2.08}O_4 + CuO$
	T peak: 144	Calculated: 19.23	
	160–215	14.22	
	215–303	22.38	
$(Cu_{0.37}Ni_{0.63})(HCOO)_2 \cdot 2H_2O$	105–174	Experimental: 18.56	$Cu_{0.2}Ni_{0.8}O$
	T peak: 156	Calculated: 19.24	
	174–199	18.46	
	199–240	20.97	
$(Cu_{0.35}Zn_{0.65})(HCOO)_2 \cdot 2H_2O$	63–147	Experimental: 19.32	$CuO + ZnO$
	T peak: 121	Calculated: 18.90	
	147–258	38.70	
$(Cu_{0.47}Cd_{0.53})(HCOO)_2 \cdot 2H_2O$	59–158	Experimental: 16.15	$CuO + CdO$
	T peak: 88	Calculated: 16.82	
	158–244	12.67	
	244–317	16.58	
	317–419	2.75	

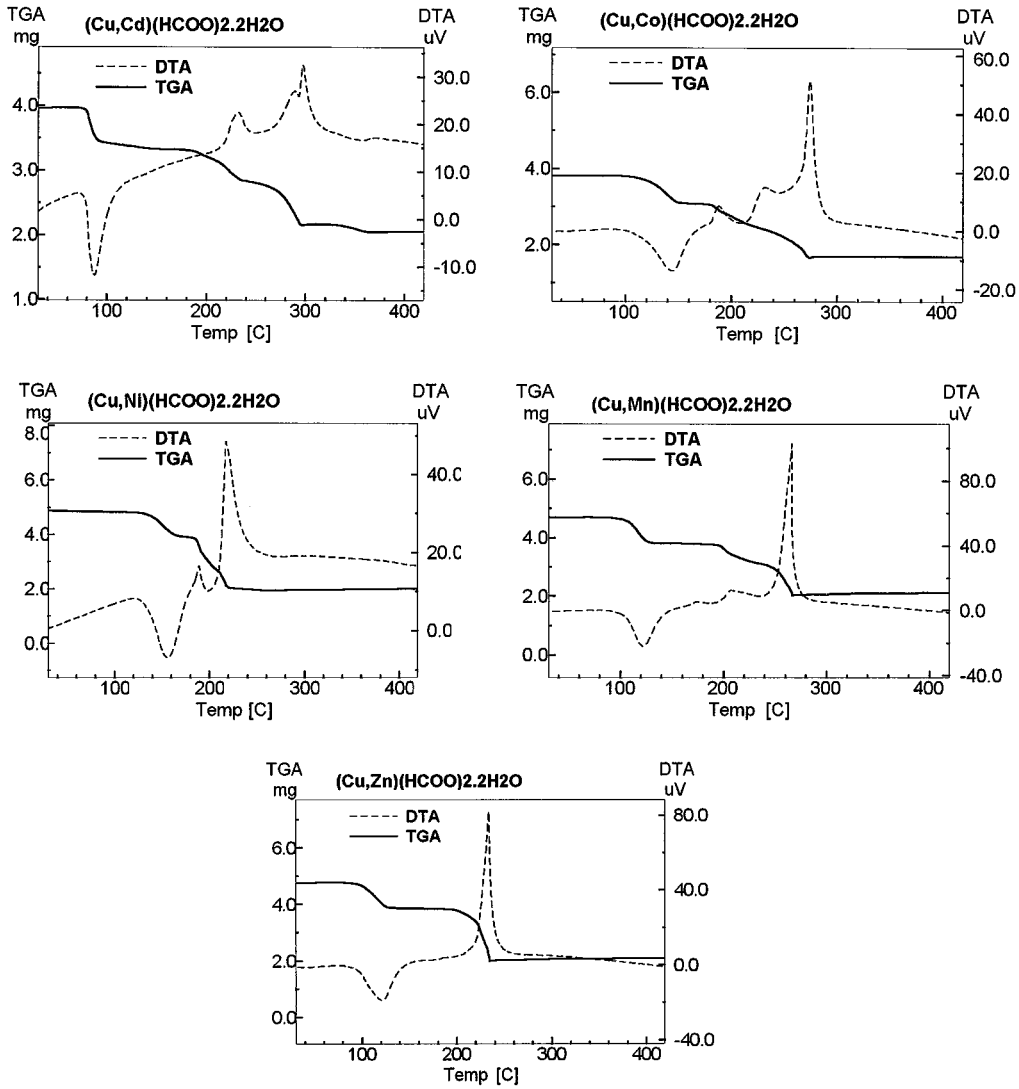

FIG. 2. TGA and DTA tracings for **(i)**, **(ii)**, **(iii)**, **(iv)**, and $M = Zn$.

coordinating oxygen atoms. The copper formate shows the lowest dehydration temperature due to the well known autocatalytic behavior (12).

This trend of the dehydration temperatures with the electronic configuration of the M ions strongly suggests that the water molecules are preferentially linked to them; otherwise a much smaller variation in dehydration temperatures ought to be expected among the different mixed formates. These findings point to site M1 as the one to be basically occupied by copper, site M2 being mainly populated by the divalent cation. This agrees with the results from single-crystal X-ray work. Besides, the latter can be correlated with some conspicuous results from TGA, viz., the surprisingly lower dehydration temperature of (iv) which could be ascribed to the weaker H-bonding interactions connecting the aqua molecule O1W to the rest of the structure.

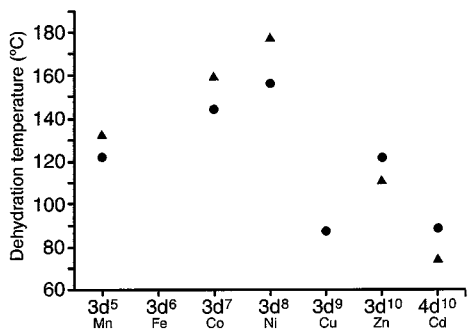

FIG. 3. Dehydration temperature for **(i)**, **(ii)**, **(iii)**, **(iv)**, and $M = Zn$ (marked ●) and for the pure M formates from which they derive, $M = Mn$, Co, Zn, and Cd (marked ▲), as a function of Md orbital electrons number. The dehydration temperature of the single formates were obtained by DTG analysis and are in agreement with those reported by Masuda (13).

The conclusions arrived at are in agreement with those of (1, 4) but not with those in (3, 5, 6); however, we believe that the results obtained from the occupation factors derived from the refinement of single crystal X-ray diffraction data as was well as the results obtained by dynamic methods as a function of temperature are a conclusive evidence that M1 is the preferential site for copper ions in mixed Cu_x–$M_{1-x}(HCOO)_2 \cdot 2H_2O$ structures.

ACKNOWLEDGMENTS

We thank Ms. Irene Fuertes for the flame absorption analysis and Ms. Mariana Rosenbuch for the EDAX analyses. The technical assistance of Ms. Alicia Petragalli is acknowledged. This research was partially supported by CONICET (PMT-PICT 0051).

REFERENCES

1. T. Ogata, T. Taga, and K. Osaki, *Bull. Chem. Soc. Jpn.* **50,** 1680 (1977).
2. D. Stoilova and S. Angelov, *J. Solid State Chem.* **82,** 60 (1989).
3. D. Stoilova and G. Gentcheva, *J. Solid State Chem.* **100,** 24 (1992).
4. D. Stoilova, St. Peter, and H. D. Lutz, *Z. Anorg. Allg. Chem.* **620,** 1793 (1994).
5. D. Stoilova, *J. Solid State Chem.* **104,** 404 (1993).
6. T. Ogata, T. Taga, and K. Osaki, *Bull. Chem. Soc. Jpn.* **50,** 1674 (1977).
7. G. M. Sheldrick, "SHELXL-97. Program for Structure Refinement." Univ of Göttingen, Germany, 1997.
8. G. Weber, *Acta Crystallogr. B* **36,** 1947 (1980).
9. International Center for Diffraction Data, "Powder Diffraction File-2, Data Base," 1997.
10. E. Nicolas-Tolentino, Z. R. Tian, H. Zhou, G. Xia, and S. L. Suib, *Chem. Mater.* **11,** 1733 (1999).
11. M. G. Ei-Shaarawy and S. A. Shama, *J. Mater. Sci.* **34,** 1229 (1999).
12. "Chemical Kinetics" (C. H. Bamford and C. F. H. Tipper, Eds.), Vol. 22, p. 213. Elsevier, Amsterdam, 1980.
13. Sapiña, M. Burgos, E. Escriva, J. V. Folgado, D. Marcos, A. Beltran, and D. Beltran, *Inorg. Chem.* **32,** 4337 (1993).
14. Y. Masuda and S. Shishido, *Thermochim. Acta* **28,** 377 (1979).